

Integrated Printed Circuit Board Device for Cell Lysis and Nucleic Acid Extraction

Lewis A. Marshall,[†] Liang Li Wu,[‡] Sarkis Babikian,[§] Mark Bachman,[§] and Juan G. Santiago^{*,||}

[†]Department of Chemical Engineering, Stanford University, Stanford, California 94305, United States

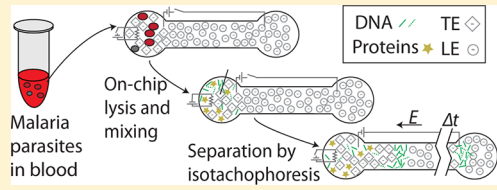
[‡]Integrated Nanosystems Research Facility, University of California, Irvine, California 92697, United States

[§]Department of Electrical Engineering and Computer Science, University of California, Irvine, California 92697, United States

^{||}Department of Mechanical Engineering, Stanford University, Stanford, California 94305, United States

S Supporting Information

ABSTRACT: Preparation of raw, untreated biological samples remains a major challenge in microfluidics. We present a novel microfluidic device based on the integration of printed circuit boards and an isotachopheresis assay for sample preparation of nucleic acids from biological samples. The device has integrated resistive heaters and temperature sensors as well as a $70\ \mu\text{m} \times 300\ \mu\text{m} \times 3.7\ \text{cm}$ microfluidic channel connecting two $15\ \mu\text{L}$ reservoirs. We demonstrated this device by extracting pathogenic nucleic acids from $1\ \mu\text{L}$ dispensed volume of whole blood spiked with *Plasmodium falciparum*. We dispensed whole blood directly onto an on-chip reservoir, and the system's integrated heaters simultaneously lysed and mixed the sample. We used isotachopheresis to extract the nucleic acids into a secondary buffer via isotachopheresis. We analyzed the convective mixing action with micro particle image velocimetry (micro-PIV) and verified the purity and amount of extracted nucleic acids using off-chip quantitative polymerase chain reaction (PCR). We achieved a clinically relevant limit of detection of 500 parasites per microliter. The system has no moving parts, and the process is potentially compatible with a wide range of on-chip hybridization or amplification assays.



Despite the advent of a wide range of on-chip assays, sample preparation remains a “weak link” in microfluidics.¹ When working with real biological or clinical samples, a microfluidic diagnostic device may have to overcome high concentrations of interfering species (e.g., proteins) to collect a relatively low concentration of target biomacromolecules, including target nucleic acids. Achieving rapid, robust sample preparation on microfluidic devices is a continuing challenge and a necessary component in developing fully integrated and useful microfluidic diagnostic devices.

To achieve nucleic acid extraction from cell samples, a microfluidic device needs to perform cell lysis (to make nucleic acids accessible) and nucleic acid extraction (to purify the nucleic acids from other cell components.) The most common way to integrate these two functions on a microchip is to use chaotropic agents for chemical cell lysis, followed by solid phase extraction.² As two examples, Chen et al. and Bienvenue et al. each applied guanidinium salts (strong chaotropic agents) to lyse cells on-chip and then used solid phase extraction (SPE) and multiple buffer exchanges and washes to extract DNA from the lysate.^{3,4} The disadvantage of the common approach of chaotropic agents and SPE is that it requires pressure-driven flow to perform the necessary buffer exchanges. This pressure-driven flow of multiple reactants often requires off-chip pumping and valve actuation or repeated manual reloading of solutions between the wash and elution steps. This leads to more design complexity and larger package size in on-chip SPE systems. We here present a microfluidic device that integrates mixing, thermal lysis of whole blood, and nucleic acid extraction

in a compact chip with no moving parts. The system uses isotachopheresis (ITP) for nucleic acid extraction and so requires no off-chip actuation except for electrical control with a voltage source. We use a fabrication method that leverages printed circuit board (PCB) technology to realize a low-cost, reconfigurable system.

Several systems have implemented and integrated heating with microfluidic devices. For example, Liu et al. used an off-chip Peltier heater coupled to a microfluidic system to perform on-chip lysis of captured *Escherichia coli* cells, followed by polymerase chain reaction (PCR).⁵ Lee et al. developed a poly(dimethylsiloxane) (PDMS) device on a glass substrate with platinum surface deposited resistive heaters.⁶ The latter device performed thermal lysis, microfluidic mixing, and PCR. However, neither device performed nucleic acid purification. Kim et al. demonstrated convective mixing and PCR in a microfluidic heating chamber but did not implement cell lysis.⁷ We know of no previous microfluidic devices that integrate on-chip mixing, thermal lysis, and nucleic acid extraction.

Nucleic acid purification is critical when processing complex samples such as whole blood. Blood has relatively high ionic strength (order 100 mM)⁸ and contains species inhibitory to DNA hybridization, protein–ligand binding, and amplification. For example, PCR is inhibited by hemoproteins, lactoferrin,

Received: September 11, 2012

Accepted: September 20, 2012

Published: October 9, 2012

immunoglobulin G, and, at sufficient ionic strength, mono- and divalent ions.⁹

ITP has been demonstrated as a purification technique for nucleic acids from blood,^{10,11} urine,¹² and cell culture.¹³ To extract nucleic acids using ITP, a complex sample mixture is introduced into a two-buffer system. The leading electrolyte (LE) buffer contains an anionic species with electrophoretic mobility higher than that of DNA. The trailing electrolyte (TE) buffer is designed to contain an anionic species with an electrophoretic mobility lower than DNA but faster than anionic impurities (cationic impurities never exit the sample reservoir). When an electric field is applied across the two buffers, an electric field gradient forms between the TE and LE, and nucleic acids quickly move to and focus at the interface. ITP is robust,¹⁴ is rapid,¹² and can be extremely selective.^{15,16} ITP does not rely on surface chemistry for species capture and is insensitive to substrate material and geometry. It is capable of preconcentrating small molecules by 10^6 -fold¹⁷ and can routinely extract and preconcentrate nucleic acids by more than 10^3 -fold in about 1 min.¹⁰ However, previous efforts to use ITP for nucleic acid extraction have required at least one off-chip sample preparation step such as mixing with lysis buffer, heating, and/or incubation with a reagent such as proteinase K.

Our PCB microfluidic device performs rapid mixing and lysis on-chip using integrated resistive heaters, and the microfluidic components allow us to perform ITP separation of nucleic acids, with results comparable to a protocol using standard off-chip lysis and a glass capillary for ITP.¹¹ The results show that ITP and PCB microfluidic devices have potential to decouple microfluidic analysis from benchtop preparation techniques.

EXPERIMENTAL SECTION

Device Fabrication. We first designed and fabricated a custom heating package for use on the PCB device. For the current work, we chose to integrate four 3.9Ω resistive heaters (32R9407 thick film resistor, Panasonic, Secaucus, NJ) with a thermistor (LM 94023 IC temperature sensor, National Semiconductor, Santa Clara, CA). The components were soldered onto a $0.2 \text{ mm} \times 3.2 \text{ mm} \times 3.2 \text{ mm}$ PCB board. The package was then encapsulated using thermal epoxy (50-3100 epoxy resin, Epoxies Etc., Cranston, RI). This yielded the final size for the heating package of $1 \text{ mm} \times 3.2 \text{ mm} \times 3.2 \text{ mm}$.

The fabrication process for our PCB microfluidic devices is shown schematically in Figure S-1 of the Supporting Information. Our devices consist of two sections: the printed circuit board layer with surface-mount components and the microfluidic layer with reagent reservoirs attached. The trace layout for the PCB layer was designed using EagleCad software (CadSoft Computer GmbH, Delray Beach, FL). Metal traces are fabricated onto the epoxy-resin (FR-4) PCB through a standard foundry service (Sierra Circuits, Inc., Sunnyvale, CA). Surface mount components were then soldered onto the board.

Polyurethane casting and stamping procedures were used to create the microfluidic layer. The PCB layer was first inserted into a frame to hold polyurethane during pouring. The device was then planarized by pouring a thin layer of mixed polyurethane monomer and curing agent (Crystal Clear 202, viscosity of 600 cps, Smooth-On Inc., Easton, PA). We placed 1 mm glass beads in this layer as spacers to define the polymer thickness. The polyurethane was allowed to cure at room temperature for 2 h. After planarization, a second polyurethane layer was fabricated separately in another container to create the fluidics. A PDMS mold was used to stamp the desired

microfluidic pattern onto the fluidic layer. For the current work, the pattern was a simple, straight channel with a depth and width of $70 \mu\text{m} \times 300 \mu\text{m}$ and length of 3.7 cm connecting the two $15 \mu\text{L}$ reservoirs. Before the microfluidic layer became fully cured, the PDMS mold was removed and both layers of polyurethane were sealed together and released from the frames. In addition, a thin layer of polyurethane-laminated poly(methyl methacrylate) (PMMA) with 4 mm access ports for the reservoirs was attached to the fluidics layer as a rigid support. Lastly, electrical connection pins were soldered in through access vias on the PCB board. The finished device is shown in Figure 1a. Detailed descriptions and characterization of the manufacturing process will be the focus of a future publication.

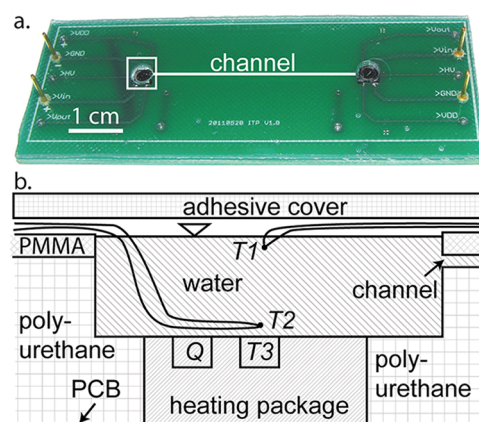


Figure 1. Hybrid PCB microfluidic device. (a) (Green) PCB substrate with surface-mounted components and (clear) polymer microfluidic layers. The channel location is highlighted using a white line for clarity. Each end-channel reservoir is integrated with a thermistor temperature sensor and heater. (b) Schematic of the cross section of the heated reservoir (outlined by the small white rectangle in part a). The thermistor (T3) and heaters lie within a 1 mm layer of thermal epoxy in the heating package. These are embedded in the 1 mm polyurethane planarization layer on the PCB substrate, above which is the polyurethane fluidic layer. The top layer of the device is 0.2 mm of stiff PMMA. Heat was applied at the embedded heater (Q). For temperature characterization, we instrumented the reservoirs with thermocouples T1 and T2, which measured temperature near the top and bottom of the liquid in the reservoir as shown.

Temperature Measurement. As shown in Figure 1b, each heater was embedded beneath the end-channel sample reservoirs in the microfluidics layer. It was activated by applying up to 200 mA to the resistive heating pins using a 1 kV maximum voltage sourcemeter (model 2410, Keithley, Cleveland, OH). The temperature was measured by supplying 3.3 V to the supply pin of the thermistor and measuring the voltage between the ground pin and the sensing pin of the thermistor. We used the voltage transfer function given by the thermistor manufacturer (see operation manual for LM 94023 IC) to calculate the thermistor temperature.

We investigated temperatures throughout the sample reservoir during heating using both the on-chip thermistor and the two free-standing 0.125 mm K-type thermocouples (Omega Inc. CHAL-005, Stamford, CT). We manually inserted the thermocouples into the reservoir, near the top and bottom surfaces, as shown schematically in Figure 1b. We recorded the thermocouple reading at 0.5 Hz using a dual thermocouple

reader and its companion software (Omega Inc., Stamford, CT).

We also recorded temperature readings from the on-chip thermistor. The on-chip thermistor and the resistive heater are separated by about 1 mm and packaged within thermal epoxy. The thermistor temperature is therefore more strongly coupled to the resistive heater than to the liquid in the reservoir. However, the reservoir structure and its contents have a significant thermal mass. To take advantage of this, we developed and implemented a pulse-modulated heating and continuous sensing method to accurately estimate the temperature in the liquid. To this end, we operated the heater using 1.4 s rectangular pulses at 8 V separated by 5.6 s at 0 V (20% duty cycle), with measured maximum currents of approximately 500 mA (about 0.8 W time-averaged power). When the heater is on, the temperature in the heater quickly and significantly exceeds the liquid temperature. When the heater is off, the temperature in the heater and the liquid quickly converge. (See the Supporting Information, Figure S-2.) We accurately estimate the temperature of the liquid by measuring the temperature to which the thermistor converges. We collected data from the on-chip thermistor using a UI2 DAQ (LabJack, Lakewood, CO) and its companion software.

Convection. Our heater provided a localized high-temperature region at the bottom of the sample reservoir (see the rectangles in Figure 4a). We characterized the thermal convective mixing caused by this localized heating using micro particle image velocimetry (micro-PIV). We filled the reservoirs with 15 μL of water seeded with 4 μm polystyrene particles doped with a proprietary red fluorescent dye with maximum excitation at 580 nm and maximum emission at 605 nm (Sigma-Aldrich, St. Louis, MO). Particles were illuminated using a mercury lamp in a BX60 epifluorescent microscope (Olympus, Center Valley, PA) using a 4 \times objective (numerical aperture 0.1) and a filter cube optimized for use with Cy3 (Omega Optics, Brattleboro, VT). Current between 0 and 180 mA was applied to the resistive heater, and images of the reservoir were captured using an intensified CCD camera (PI-MAX: 512, Princeton Instruments, Trenton, NJ) at a 200 ms exposure time. We used custom micro-PIV software to analyze the images. We used the standard (iterative) super-resolution approach¹⁸ with 30 pixel square (final) interrogation regions and 200 ms time-between-frames.

Lysis and Separation. We demonstrated the efficacy of our devices using a series of heating, lysis, and ITP-based extraction experiments, with chemistry similar to that described by Marshall et al.¹¹ As with that previous work, we here were interested in sample preparation of pathogen nucleic acids from malaria parasites spiked into whole blood samples (malaria parasites require more aggressive lysing than host leukocytes). The protocol we used for on-chip lysis and ITP extraction is shown in Figure 2. We modified our protocol from the previous work by reducing the ionic strength of the buffers and changing the surfactant to Tween 20. Blood was mixed directly into a single mixture which served as both lysis buffer and trailing electrolyte buffer (instead of using separate lysis and ITP steps).

Briefly, we filled the channel and one reservoir with an aqueous leading electrolyte (LE) containing 50 mM Tris titrated with HCl to pH 8.2 with 0.1% Tween 20 and 10 μM SYTO 60 fluorescent dye (excitation at 652 nm, emission at 678 nm). We then emptied the opposite reservoir with vacuum and refilled it with 13 μL of an aqueous trailing electrolyte (TE)

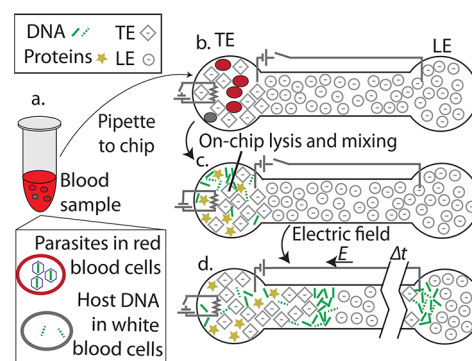


Figure 2. Schematic of malaria extraction protocol. (a) Malaria parasites were spiked into whole blood to provide a realistic sample. (b) The blood was pipetted directly into the on-chip reservoir, which was filled with the combined lysis and TE buffer. (c) This reservoir was sealed and heat was applied using the on-chip resistive heater. (d) After lysis, the heating was turned off and the electric field was applied between the two reservoirs. Nucleic acids were extracted and purified into the LE reservoir, where they were collected for off-chip analysis.

buffer containing 50 mM Tris titrated with 50 mM HEPES and 1 μL of proteinase K (Invitrogen, Carlsbad, CA). We pipetted 1 μL of whole blood spiked with *Plasmodium falciparum* parasites cultured in human erythrocytes. We then sealed both reservoirs with 5 mm \times 5 mm squares of PCR-plate adhesive film (Bio-Rad, Hercules, CA) and applied 180 mA to both resistive heaters for 3 min. After this, the reservoirs were allowed to cool for 1 min (to approximately 40 $^{\circ}\text{C}$), after which the adhesive seals were removed. We inserted platinum electrodes into both reservoirs and applied +500 V in the LE versus the ground electrode in the TE to initiate ITP. We monitored ITP by measuring current and by visualizing SYTO 60 fluorescence using the epifluorescent microscope and a filter cube optimized for Cy5 dye (Semrock, Lake Forest, IL). When the ITP interface reached the LE reservoir, we deactivated the voltage and then mixed and collected the contents of the LE reservoir for later, off-chip analysis. The PCB device had negligible autofluorescence in the SYTO 60 emission spectrum of about 650–700 nm. At shorter wavelengths (e.g., the emission spectrum of SYBR Green DNA-specific fluorescent dye), the PCB substrate exhibited strong background fluorescence.

To verify that cells were being lysed during the on-chip heating, we performed manual cell counting of samples before and after cell lysis using disposable hemocytometers (Cell-Vu, New York, NY). We fluorescently labeled the malaria parasites using DNA-specific SYBR Gold dye. This allowed easy differentiation between DNA-free erythrocytes and DNA-containing malaria parasites.¹⁹ The cell counting protocol is given in section S-5 on the Supporting Information. We used the cell counts before and after the lysis protocol to calculate the lysis efficiency, defined as

$$\text{lysis efficiency} = 1 - \frac{\text{lysed cell count}}{\text{unlysed cell count}}$$

Polymerase Chain Reaction. We validated the purity and efficiency of our integrated and automated on-chip lysis and extraction using off-chip quantitative polymerase chain reaction (qPCR). These experiments confirmed the presence of the target nucleic acids and successful extraction from PCR-inhibiting chemical species in blood. For these experiments, we added 4 μL of DNA extracted with our PCB microfluidic device

directly into a PCR tube containing 10 μL of Fast SYBR Green PCR master mix (Applied Biosystems, Carlsbad, CA), 6 μL of DNase free water, and 150 nM each of forward and reverse primers. We also performed positive control experiments in which the template was DNA extracted from the same malaria parasites using a commercial solid phase extraction kit (Qiagen, Valencia, CA). We used validated primers for the circumsporozoite protein gene in *Plasmodium falciparum*²⁰ (PFCS79, 5'-GGAAGTCGTCAAACACAAG-3', and PFCS233, 5'-CCATCATCATTTTCTCCAAG-3'). Analysis was performed in a miniOpticon qPCR thermocycler (Bio-Rad, Hercules, CA) with the following thermal profile: 20 s initial hold at 95 °C and 40 cycles composed of 3 s denaturation at 95 °C and 30 s annealing and extension at 60 °C. We obtained post-PCR dissociation curves using the same instrument.

RESULTS AND DISCUSSION

Reservoir Temperature. We measured both transient and steady-state temperatures in the reservoir upon application of current to the resistive heater, as summarized in Figure 3. The

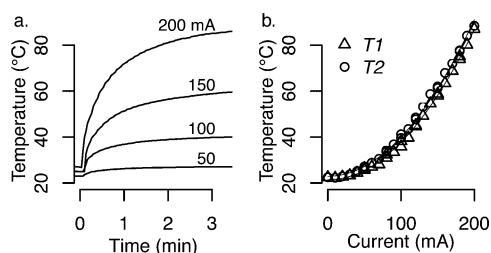


Figure 3. Measurements of on-chip heating temperatures. (a) Transient temperature profiles in the reservoir (T1) at various applied currents. Temperature approaches steady state within about 3 min. (b) Steady state temperatures as a function of applied current. Temperature was quantified using thermocouples T1 and T2 simultaneously. We here defined steady state as the temperature at which the reservoir was changing less than 0.5 °C/s. The difference between the T1 and T2 measured temperatures was less than about 5 °C, indicating vigorous mixing by thermal convection. Quadratic trend lines are plotted to show the relation between applied power and steady state temperature.

device approaches steady state temperature within 3 min and can achieve temperatures ranging from room temperature to 90 °C (T1), depending on applied current. The resistive heater can sustain currents up to 200 mA; higher currents damage the device. The steady-state reservoir temperature is proportional to the square of the applied current, as shown by the quadratic fit lines in Figure 3b. This is consistent with a steady-state model in which power is supplied to the reservoir by Joule heating in the resistor and dissipated to the environment at a rate proportional to the temperature difference between the liquid and the environment. A simple model for this process is as follows:

$$Q_{\text{in}} = Q_{\text{out}}$$

$$Q_{\text{in}} = IV = I^2R$$

$$Q_{\text{out}} = hA(T - T_0)$$

Here, Q_{in} and Q_{out} are the power input and output, I is the applied current, V is the voltage drop across the resistive heaters, and R is the resistance. h is an effective heat transfer

coefficient of heat rejection to the environment, A is the surface area of the reservoir, and $T - T_0$ is the difference between the (approximately uniform) reservoir temperature and room temperature. These equations can be combined and rearranged as follows:

$$(T - T_0) = I^2 \frac{R}{hA}$$

This simple analysis shows that reservoir temperature should be approximately proportional to the square of applied current.

We demonstrated the efficacy of using our embedded thermistor and pulsed heating method to measure the temperature of the liquid in the reservoir. We obtained simultaneous measurements of the thermocouple T1 and the embedded thermistor. Example simultaneous temperature traces of these two measurements are shown in the Supporting Information (see Figure S-2). The temperature measured by the thermistor equilibrated to within about 5 °C of the measured water temperature at the end of each 5.6 s deactivated current interval. The on-chip thermistor was therefore able to fairly accurately measure the reservoir temperature.

Thermal Convection. We used micro-PIV^{21,22} to quantify the thermal convection-generated velocity fields in the reservoir. We placed the focal plane of our 0.4 \times objective (numerical aperture 0.1) 0.1 mm from the top surface of the 1.2 mm deep volume of liquid in the sample reservoir. A representative flow field is shown in Figure 4a. We quantified

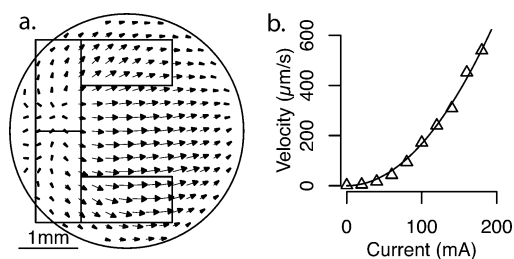


Figure 4. Convective mixing data. (a) Micro particle image velocimetry measurements of convective flow inside the reservoir during heating. Flow was visualized by seeding with 1 μm fluorescent beads and placing the focal plane 0.1 mm from the top of the 1.2 mm deep liquid level in the reservoir. Images were analyzed using custom micro-PIV software. Rectangles show the locations of the four embedded resistive heaters. (b) Maximum (in-plane) convective mixing velocity as a function of current applied to the on-chip heater. We show a quadratic fit line with the data.

flow fields at a variety of applied currents. At a heating power of 0.58 W (180 mA applied current), we recorded in-plane flow velocities of up to 600 $\mu\text{m}/\text{s}$ (as shown in Figure 4b). The flow velocities were steady and showed a clear pattern with heated liquid rising from the off-center heater at the bottom of the reservoir and circulating away and then downward near the far edges of the reservoir (see Figure 4). Although not shown here, we observed the complementary flow toward the heater when we analyzed flow velocities near the bottom of the reservoir. Repeated experiments show that the flow patterns were repeatable and the process ergodic. The flow velocities therefore imply that, during the 3 min lysis step, fluid particles traversed the reservoir approximately 20 times, allowing for efficient mixing with the lysis buffer. We estimate the Rayleigh numbers (Ra), defined as $(g\beta\Delta TL^3)/(\nu\alpha)$, where g is the

gravitational acceleration, β is the thermal expansion coefficient of water, L is the height of the reservoir, ν is the kinematic viscosity of water, α is the thermal diffusivity, and ΔT is the measured temperature differences between the top and bottom of the reservoir. These Ra values vary between 12 and 1200 (as shown in the Supporting Information in Figure S-3) for reservoir temperature differences ($T_2 - T_1$) ranging from 0.1 to 4.5 °C. These Ra are below the theoretical critical threshold value of 1710 for convection between two uniform-temperature flat plates.²³ We hypothesize that the strongly asymmetric and localized heating provided by our off-center heater design promoted strong circulation at lower Ra . We recommend that the study of geometries for achieving strong on-chip thermal convection and mixing at low temperature differences and in small geometries would be a good contribution to the microfluidics field.

Temperature-Induced Pressure Driven Flow. As described earlier, our protocol used an adhesive seal to cover the reservoir during heating. We observed that heating a single, covered reservoir connected to a channel caused a finite amount of pressure-driven flow out from that reservoir. This flow is likely caused by the increased vapor pressure in the reservoirs at elevated temperature. We developed a simple model for this flow based on thermodynamic equilibrium estimates of the partial pressures in the gas layer at the top of the sealed reservoir. We present some observations based on this model in section S-4 and Figure S-4 in the Supporting Information. We hope to validate this model and present it in a future publication. The analysis shows that pressure driven flow is minimized when both the inlet and outlet reservoirs are heated simultaneously such that the temperature in both reservoirs is equal and when the initial gas space is as small as possible. To reduce heat-induced pressure-driven flow in our experiments, we applied equal currents to both reservoir heaters and filled the reservoirs equally to within 1 μL of their capacities.

Lysis and Separation. We quantified the lysis efficiency of our system and compared it to off-chip lysis methods. A description of the lysis efficiency measurement method used here is in section S-5 of the Supporting Information. Figure 5 summarizes our lysis results. Our on-chip lysis approach achieves up to 90% lysis efficiency at 180 mA applied current. We chose to operate our heater at 180 mA for the current extraction experiments.

We visualized the focused and purified nucleic acids zone during ITP extraction using SYTO 60 red DNA-specific dye. A

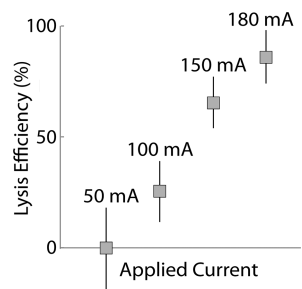


Figure 5. Measurements of lysis efficiency of malaria parasites in human blood. Cells were lysed at four applied currents in the on-chip heating system integrated within our PCB microfluidic device. Each measurement was repeated $N = 14$ –18 times. Uncertainty bars indicate 95% confidence intervals on the means.

representative image of the extracted total nucleic acids in the microfluidic channel as they exit into the downstream reservoir is shown in Figure 6.

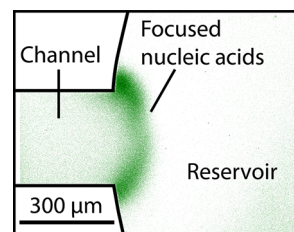


Figure 6. Example image of ITP zone of extracted DNA as it exits the channel and enters the downstream (leading electrolyte) reservoir of our PCB microfluidic device. Nucleic acids were labeled with SYTO 60. The ITP zone curved outward as shown when the current lines fringed outward.

Polymerase Chain Reaction. The results of our off-chip qPCR validation of the purity and amount of extracted nucleic acids are summarized in Figure 7. Our qPCR experiments show

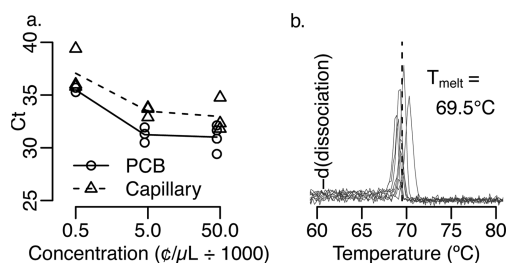


Figure 7. Off-chip qPCR measurements to show the purity, quantity, and PCR-compatibility of the nucleic acid extracted using our integrated device. (a) qPCR threshold cycles of the extracted nucleic acids as a function of parasite concentration in the original infected blood sample dispensed into the chip. PCR primers targeted the circumsporozite gene in *P. falciparum*. We observed no amplification in negative control reactions that contained unprocessed infected blood samples and nuclease-free water as template. Data from our PCB-device extractions (circles, solid line) is compared to similar data gathered using the same ITP chemistry and ITP process but with off-chip lysis and separation in a glass capillary (triangles, dotted line). Adapted from ref 11. Copyright 2011 American Chemical Society. Line segments connect mean threshold cycles. (b) Nine dissociation curves of the amplified PCR product of the extracted DNA. Dissociation temperatures cluster closely around the theoretical melting temperature for the target amplicon, shown as a vertical dotted line. This melting temperature matches positive controls using template DNA extracted from infected blood samples by a commercial solid phase extraction system (Qiagen, Valencia, CA).

amplification down to 500 parasites per microliter. In Figure 7a, we compare our qPCR threshold cycles to those of Marshall et al.,¹¹ who used a similar ITP extraction method in a free-standing borosilicate glass capillary. The resulting trends are in close agreement, although they should not be quantitatively compared because they were performed on different qPCR machines. We constructed a calibration curve for DNA concentration as a function of the qPCR threshold cycle to estimate the extraction efficiency of our device. These estimates and experiments are described in the Supporting Information (see section S-6 and Figure S-5).

Figure 7b shows dissociation data for the PCR product from nine samples. The product dissociates near the theoretical

melting temperature, 69.5 °C, for our target sequence, consistent with our conclusion that we amplified the correct PCR product. The nine amplicon samples showed a standard deviation of 0.4 °C from the mean melting temperature of 69.4 °C. The 69.5 °C theoretical value was predicted using mfold thermodynamic simulation software (RNA Institute, University of Albany).²⁴

CONCLUSION

We demonstrated the operation of a PCB microfluidic device where we directly dispense 1 μ L of unprocessed whole blood into a chip and automatically mix, lyse, and extract PCR-compatible nucleic acid into a downstream reservoir. The chip uses integrated heaters and temperature sensors to achieve controlled temperatures of up to 90 °C in a 15 μ L reservoir. We achieved lysis using a combined lysis and trailing electrolyte ITP buffer and localized heating. Localized heating causes rapid thermal-convection-driven mixing and promotes lysis. After lysis, the heater is deactivated and ITP is used to automatically extract and purify PCR-compatible nucleic acids into a downstream reservoir. The chip can operate with no manual steps after dispensing blood, and the system has no moving parts. The device also uses no off-chip pumps, valves, or pressure sources.

The integration of electronics and microfluidics in PCB devices demonstrates that it is possible to break the heavy and nearly ubiquitous dependence of microfluidics on off-chip, benchtop-scale sample preparation methods for complex biological samples. By bringing more operations on-chip, we can begin to create robust, practical lab-on-chip devices for medical care.

ASSOCIATED CONTENT

Supporting Information

Additional information as noted in text. This material is available free of charge via the Internet at <http://pubs.acs.org>.

AUTHOR INFORMATION

Corresponding Author

*E-mail: juan.g.santiago@stanford.edu.

Notes

The authors declare no competing financial interest.

ACKNOWLEDGMENTS

We thank Prof. Niaz Banaei and Dr. Ellen Yeh for providing *P. falciparum* samples. This work was supported in part by the Defense Advanced Research Projects Agency (DARPA) N/MEMS S&T Fundamentals Program under Grant Number N66001-1-4003 issued by the Space and Naval Warfare Systems Center Pacific (SPAWAR) to the Micro/Nano Fluidics Fundamentals Focus (MF3) Center. J.G.S. and L.A.M. also gratefully acknowledge funding from DARPA under Grant Number HR0011-12-C-0080 as well as funding from the Gates Foundation under Contract Number OPP1007350 GCE.

REFERENCES

- (1) Mariella, R. *Biomed. Microdevices* **2008**, *10*, 777–784.
- (2) Wen, J.; Legendre, L. A.; Bienvenue, J. M.; Landers, J. P. *Anal. Chem.* **2008**, *80*, 6472–6479.
- (3) Chen, X.; Cui, D.; Liu, C.; Li, H.; Chen, J. *Anal. Chim. Acta* **2007**, *584*, 237–243.
- (4) Bienvenue, J. M.; Duncalf, N.; Marchiarullo, D.; Ferrance, J. P.; Landers, J. P. *J. Forensic Sci.* **2006**, *51*, 266–273.

- (5) Liu, R. H.; Yang, J.; Lenigk, R.; Bonanno, J.; Grodzinski, P. *Anal. Chem.* **2004**, *76*, 1824–1831.
- (6) Lee, C.-Y.; Lee, G.-B.; Lin, J.-L.; Huang, F.-C.; Liao, C.-S. *J. Micromech. Microeng.* **2005**, *15*, 1215–1223.
- (7) Kim, S. J.; Wang, F.; Burns, M. A.; Kurabayashi, K. *Anal. Chem.* **2009**, *81*, 4510–4516.
- (8) Allport-Settle, M. *Investigations Operations Manual: FDA Field Inspection and Investigation Policy and Procedure Concise Reference*; PharmaLogika, 2010.
- (9) Bessetti, J. An Introduction to PCR Inhibitors. In *Promega Corporation Profiles in DNA*, 2007, *10*(1), 9–10. <http://www.promega.com/resources/articles/profiles-in-dna/2007/an-introduction-to-pcr-inhibitors/>. Accessed October 2012.
- (10) Persat, A.; Marshall, L. A.; Santiago, J. *Anal. Chem.* **2009**, *81*, 9507–9511.
- (11) Marshall, L. A.; Han, C. M.; Santiago, J. G. *Anal. Chem.* **2011**, *83*, 9715–9718.
- (12) Bercovici, M.; Kaigala, G.; Mach, K.; Han, C.; Liao, J.; Santiago, J. *Anal. Chem.* **2011**, *83*, 4110–4117.
- (13) Schoch, R. B.; Ronaghi, M.; Santiago, J. G. *Lab Chip* **2009**, *9*, 2145.
- (14) Boček, P. *Analytical Isotachopheresis*; VCH: Weinheim, Germany, 1988.
- (15) Persat, A.; Chivukula, R. R.; Mendell, J. T.; Santiago, J. G. *Anal. Chem.* **2010**, *82*, 9631–9635.
- (16) Persat, A.; Santiago, J. G. *Anal. Chem.* **2011**, *83*, 2310–2316.
- (17) Jung, B.; Bharadwaj, R.; Santiago, J. G. *Anal. Chem.* **2006**, *78*, 2319–2327.
- (18) Keane, R. D.; Adrian, R. J.; Zhang, Y. *Meas. Sci. Technol.* **1995**, *6*, 754–768.
- (19) Smilkstein, M.; Sriwilajaroen, N.; Kelly, J.; Wilairat, P.; Riscoe, M. *Antimicrob. Agents Chemother.* **2004**, *48*, 1803–1806.
- (20) Wooden, J.; Kyes, S.; Sibley, C. *Parasitol. Today* **1993**, *9*, 303–305.
- (21) Santiago, J.; Wereley, S.; Meinhart, C.; Beebe, D.; Adrian, R. J. *Exp. Fluids* **1998**, *25*, 316–319.
- (22) Wereley, S. T.; Meinhart, C. D. *Annu. Rev. Fluid Mech.* **2010**, *42*, 557–576.
- (23) Akiyama, M.; Hwang, G.; Cheng, K. *J. Heat Transfer* **1971**, *93*, 335–341.
- (24) Zuker, M. *Nucleic Acids Res.* **2003**, *31*, 3406–3415.